Journal of Macromolecular Science, Part A
Publication details, including instructions for authors and subscription information:
http://www.informaworld.com/smpp/title~content=t713597274

Poly(acrylate-*b*-styrene-*b*-isobutylene-*b*-styrene-*b*-acrylate) Block Copolymers via Carbocationic and Atom Transfer Radical Polymerizations

Robson F. Storey[a]; Adam D. Scheuer[a]; Brandon C. Achord[a]
[a] School of Polymers and High Performance Materials, The University of Southern Mississippi, Hattiesburg, Mississippi, USA

To cite this Article Storey, Robson F. , Scheuer, Adam D. and Achord, Brandon C.(2006) 'Poly(acrylate-*b*-styrene-*b*-isobutylene-*b*-styrene-*b*-acrylate) Block Copolymers via Carbocationic and Atom Transfer Radical Polymerizations', Journal of Macromolecular Science, Part A, 43: 10, 1493 — 1512
To link to this Article: DOI: 10.1080/10601320600896645
URL: http://dx.doi.org/10.1080/10601320600896645

Journal of Macromolecular Science®, Part A: Pure and Applied Chemistry, 43:1493–1512, 2006

ISSN 1060-1325 print/1520-5738 online
DOI: 10.1080/10601320600896645

Poly(acrylate-*b*-styrene-*b*-isobutylene-*b*-styrene-*b*-acrylate) Block Copolymers via Carbocationic and Atom Transfer Radical Polymerizations

ROBSON F. STOREY, ADAM D. SCHEUER, AND BRANDON C. ACHORD

School of Polymers and High Performance Materials, The University of Southern Mississippi, Hattiesburg, Mississippi, USA

A series of polyacrylate-polystyrene-polyisobutylene-polystyrene-polyacrylate (X-PS-PIB-PS-X) pentablock terpolymers (X = poly(methyl acrylate) (PMA), poly(butyl acrylate) (PBA), or poly(methyl methacrylate) (PMMA)) was prepared from poly (styrene-b-isobutylene-b-styrene) (PS-PIB-PS) block copolymers (BCPs) using either a Cu(I)Cl/1,1,4,7,7-pentamethyldiethylenetriamine (PMDETA) or Cu(I)Cl/tris[2-(dimethylamino)ethyl]amine (Me_6TREN) catalyst system. The PS-PIB-PS BCPs were prepared by quasiliving carbocationic polymerization of isobutylene using a difunctional initiator, followed by the sequential addition of styrene, and were used as macroinitiators for the atom transfer radical polymerization (ATRP) of methyl acrylate (MA), n-butyl acrylate (BA), or methyl methacrylate (MMA). The ATRP of MA and BA proceeded in a controlled fashion using either a Cu(I)Cl/PMDETA or Cu(I)Cl/Me_6TREN catalyst system, as evidenced by a linear increase in molecular weight with conversion and low PDIs. The polymerization of MMA was less controlled. ^{1}H-NMR spectroscopy was used to elucidate pentablock copolymer structure and composition. The thermal stabilities of the pentablock copolymers were slightly less than the PS-PIB-PS macroinitiators due to the presence of polyacrylate or polymethacrylate outer block segments. DSC analysis of the pentablock copolymers showed a plurality of glass transition temperatures, indicating a phase separated material.

Keywords carbocationic polymerization, atom transfer radical polymerization, poly(methyl acrylate-*b*-styrene-*b*-isobutylene-*b*-styrene-*b*-methyl acrylate), block copolymer, block terpolymer

Introduction

Living polymerizations represent the most elegant and powerful method for the creation of block and graft copolymers with well defined structures and narrow polydispersites (PDI). Many chain polymerizations formerly thought to be inherently non-living, for example, carbocationic and radical, have been converted into quasi-living or controlled polymerizations through better understanding and control of polymerization kinetics. The

Received May 2006; Accepted June 2006.
Address correspondence to Robson F. Storey, The University of Southern Mississippi, 118 College Dr. #10076, Hattiesburg, MS 39406, USA. Tel.: 604-266-4879 (office); Fax: 601-266-5635; E-mail: robson.storey@usm.edu

characteristic feature of these newly developed polymerizations that imparts "livingness" is an equilibrium between active and reversibly terminated (dormant) chain ends, such that the former exist in a concentration many orders of magnitude lower than the latter.

Using living/controlled polymerization techniques, the traditional approach toward block copolymers involves the method of sequential monomer addition; however, one is limited with regard to monomer selection since all monomers involved must be amenable to the particular process, for example, carbocationic polymerization, that is being employed. The range of possible block copolymers can be expanded tremendously if two or more different living/controlled polymerization techniques can be combined. This becomes possible if an end group of the first polymer block can be provided with a functional group that is an efficient initiator for the living/controlled polymerization technique to be used for the subsequent block. This general methodology is termed site transformation.

Polyisobutylene (PIB) is a fully saturated polyolefin that can be prepared only through carbocationic polymerization. The conditions necessary for its quasi-living polymerization are well established (1–3), and a variety of block copolymers has been prepared using either direct sequential monomer addition or diphenylethylene capping followed by sequential monomer addition (4). PIB possesses high chemical, thermal, and oxidative stability, superior dampening and barrier properties, and excellent biocompatibility in medical applications such as controlled drug delivery (5). Because of these outstanding properties, there has been considerable interest in the creation of new PIB-based block and graft copolymers using a variety of methods including site transformation (6–10), grafting-from (11, 12), and grafting-through approaches (13).

A particularly facile site transformation method for creating PIB-based block copolymers involves the *in situ* end capping of quasi-living PIB with a few styrene monomer units. This results in PIB that is end-capped with *sec*-benzyl chloride groups, which are initiating moieties for atom transfer radical polymerization (ATRP). A-B-A triblock copolymers containing styrene (14, 15), *p*-acetoxystyrene (15), methyl acrylate (MA) (14), MMA (14), and isobornyl methacrylate (14) outerblocks (A) and PIB center blocks (B) have been synthesized via ATRP using *sec*-benzyl chloride-capped PIB macroinitiators. The major advantage of this technique is that no additional synthetic manipulations are required to render PIB effective as a macroinitiator.

If, instead of simply capping the intermediate PIB block with just a few styrene monomer units, a polystyrene block of significant length is created, then subsequent application of ATRP can lead to terpolymers. Storey et al. recently used this method to synthesize poly(*tert*-butyl acrylate-*b*-styrene-*b*-isobutylene-*b*-styrene-*b*-*tert*-butyl acrylate) block terpolymers (16), which were modified by post-polymerization cleavage of the *tert*-butyl ester side chains to yield poly(acrylic acid) outer blocks. The resulting amphiphilic pentablock terpolymers were found to possess interesting triphasic morphologies, thermal properties, and selective permeabilities (17).

This paper details the synthesis and thermal characterization of block terpolymers derived from PIB-PS block copolymer macroinitiators, possessing either a PIB-PS-X (X = poly(methyl acrylate) (PMA)) or X-PS-PIB-PS-X structure (X = PMA, poly(butyl acrylate) (PBA), or poly(methyl methacrylate) (PMMA)). The general synthesis of the X-PS-PIB-PS-X pentablock terpolymers is shown in Scheme 1. This method represents a facile way to prepare multiblock terpolymers, which otherwise could not be obtained, using a combination of quasi-living carbocationic polymerization (QCP) and ATRP; a particular advantage is that the intermediate PS-PIB-PS copolymers inherently possess an ATRP initiating chain-end, thereby rendering unnecessary any site-transformation

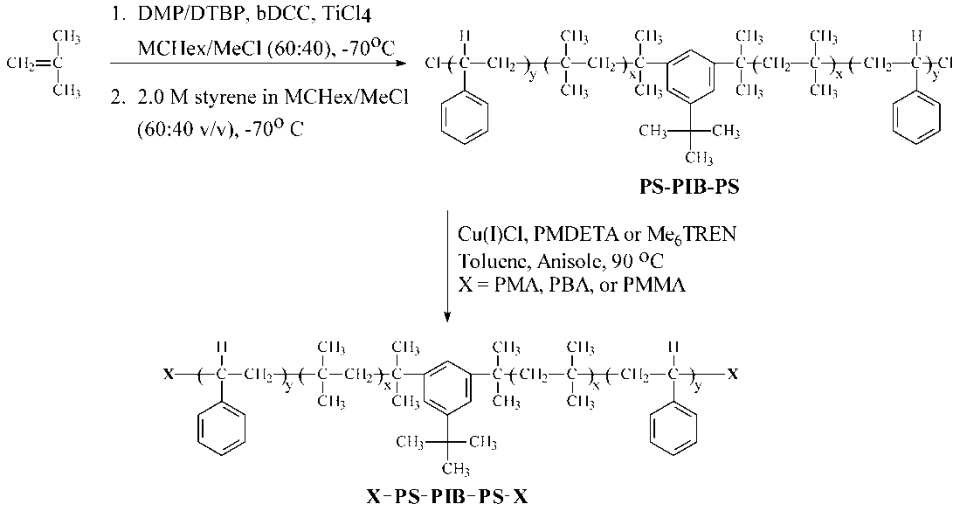

Scheme 1. General synthesis scheme for polyacrylate-PS-PIB-PS-polyacrylate pentablock terpolymers.

reactions. Incorporation of a third block segment into PS-PIB-PS block copolymers can lead to potentially useful materials with unique properties and morphologies.

Experimental

Materials

The preparation of 5-*tert*-butyl-1,3-bis(2-chloro-2-propyl)benzene (bDCC) has been previously reported (18). Isobutylene (IB) and CH_3Cl (MeCl) (both BOC, 99.5%) were dried through columns packed with $CaSO_4$ and $CaSO_4$/4 Å molecular sieves, respectively. Methyl acrylate (MA, 99%), *n*-butyl acrylate (BA, 99%), methyl methacrylate (MMA, 99%), and 2,6-di-*tert*-butyl pyridine (DTBP, 97%) were all purchased from Aldrich Chemical Co. and distilled from CaH_2 under reduced pressure. Cu(I)Cl (99+%, purified), $TiCl_4$ (99.9%, packaged under N_2 in SureSeal bottles), 2,6-dimethylpyridine (DMP, 99+%), anhydrous methylcyclohexane (MCHex, 99+%), anhydrous methanol (MeOH, 99.8%), anisole (99%), formaldehyde (37 wt% solution in water), formic acid (95–97%), and tris(2-aminoethyl)amine (96%), DOWEX®MSC-1 macroporous ion-exchange resin (Dowex sodium, strong cation, 20–50 mesh), and aluminum oxide (alumina, standard grade, activated, neutral, Brockmann I, ~150 mesh, 58 Å) were all used as received from Aldrich Chemical Co. 1,1,4,7,7-Pentamethylenetriamine (PMDETA) (99+%) and toluene (anhydrous, 99.8%), obtained from Aldrich Chemical Co., were deoxygenated by sparging with dry $N_{2(g)}$ for 30 min before use. Tris[2-(dimethylamino)ethyl] amine (Me_6TREN) was synthesized using a modification of a previously reported procedure (19) and was sparged with dry $N_{2(g)}$ for 30 min before use.

Instrumentation

Size-Exclusion Chromatography (SEC). Molecular weights and polydispersities (PDIs) of polymers were determined using a SEC system consisting of a Waters Alliance 2690

Separations Module, an on-line multi-angle laser light scattering (MALLS) detector (MiniDAWN™, Wyatt Technology Inc.) and an interferometric refractometer (Optilab DSP™, Wyatt Technology Inc.), as previously described (20). Freshly distilled THF served as the mobile phase and was delivered at a flow rate of 1.0 mL/min. Sample concentrations were 5 mg/mL in freshly distilled THF, and the injection volume was 100 μL. The detector signals were simultaneously recorded using ASTRA™ software (Wyatt Technology Inc.), and absolute molecular weights were determined by MALLS using a dn/dc value calculated from the signal response of the Optilab DSP and assuming 100% mass recovery from the columns.

NMR Spectroscopy. Solution ^{1}H-NMR spectra were obtained on a Varian Unity 300 MHz spectrometer using 5 mm o.d. tubes with sample concentrations of 5–7% (w/v) in deuterated chloroform ($CDCl_3$) (Aldrich Chemical Co.) containing 0.03% (v/v) tetramethylsilane as an internal reference. The ^{1}H-NMR spectra were the Fourier transformation of 32 transients.

Real-Time FT-IR ATR Spectroscopy. A ReactIR 1000 reaction analysis system (light conduit type) (ASI Applied Systems, Millersville, MD), equipped with a DiComp (diamond composite) insertion probe, a general-purpose type PR-11 platinum resistance thermometer, and CN76000 series temperature controller (Omega Engineering, Stamford, CT), was used to collect spectra of the polymerization components and monitor reactor temperature in real time as previously described (21). The light conduit and probe were contained within a glove box (MBraun Labmaster 130), equipped with a hexane/heptane cold bath.

Differential Scanning Calorimetry (DSC). Thermal transitions of BCPs were studied using a Mettler-Toledo thermal analysis workstation equipped with a DSC 822e. Cooling and heating scans of samples weighing 10–16 mg were run over the temperature range −100 to 150°C at 10°C/min under a constant $N_{2(g)}$ flow of 20 mL/min. Data analysis was performed using Star e2/2 software, and the glass transition temperature, T_g, was taken as the temperature corresponding to the well-defined minimum in the first derivative curve, i.e., the inflection point.

Thermogravimetric Analysis. Thermogravimetric analysis was performed on a Mettler-Toledo TGA850 instrument in conjunction with a Mettler thermal analysis workstation. Sample sizes were between 5 and 20 mg. The temperature was raised from 30 to 800° C at a heating rate of 10°C/min under a nitrogen atmosphere.

Synthesis of PS-PIB-PS ATRP and PIB-PS Macroinitiators

The following is a representative procedure for the synthesis of the PS-PIB-PS BCPs. The DiComp probe was inserted into a 1000 mL 4-necked round bottom flask equipped with a temperature probe and stirring shaft with a Teflon paddle. The reactor was placed into the heptane/hexanes bath and allowed to equilibrate to −70°C. Into the flask were charged 374 mL MCHex (−70°C), 0.875 g (3.05×10^{-3} mol) *t*-Bu-*m*-DCC, 250 mL MeCl (−70°C), 16 μL (7.1×10^{-4} mol) DTBP, and 24 μL (2.1×10^{-3} mol) DMP. This mixture was allowed to stir for 15 min, after which a background spectrum was collected. Once the background spectrum was obtained, baseline spectra were collected after which 64 mL (8.0×10^{-1} mol) IB (−70°C) was added to the flask. Several

monomer baseline spectra were obtained and 2.25 mL (2.05×10^{-2} mol) $TiCl_4$ (neat and at room temperature) was injected into the flask. Once the IB conversion was >99% (t = 141 min), a 1–2 mL aliquot was removed from the reaction vessel and added to 10 mL of prechilled MeOH. The molar concentrations of the reaction components were as follows: $[IB]_0 = 1.2$ M, $[bDCC]_0 = 4.4 \times 10^{-3}$ M, $[2,6\text{-DTBP}]_0 = 1.0 \times 10^{-3}$ M, $[DMP]_0 = 3.0 \times 10^{-3}$ M, and $[TiCl_4]_0 = 3.0 \times 10^{-2}$ M (M_n = 15,800 PDI = 1.04).

After the consumption of IB, the instrument was reset to monitor the disappearance of styrene (907 cm^{-1}) and several baseline spectra were collected. After this, a prechilled (−70°C) solution of 43 mL (3.8×10^{-1} mol) styrene in 88 mL MCHex and 76 mL MeCl was added to the reactor. When the styrene conversion reached ~50%, 50 mL prechilled MeOH was added to the reactor. The polymer was precipitated into a 10× volume excess of MeOH and dried in a vacuum oven at 25°C. The molar concentration of styrene in the charge and in the total reaction was 1.8 and 4.2×10^{-1} M, respectively. The completed PS-PIB-PS triblock copolymer had M_n = 22,900 g/mol and PDI = 1.14. The PIB-PS diblock macroinitiator was synthesized using a similar procedure, except that the monofunctional initiator, TMPCl, was used instead of bDCC.

Synthesis of Poly(methyl acrylate)-PS-PIB-PS-Poly(methyl acrylate) Pentablock Copolymers by ATRP

The following is a representative procedure for the ATRP of MA using a PS-PIB-PS macroinitiator; a similar procedure was used for the polymerization of BA and MMA. Into a ground-glass Kjeldahl-style Schlenk flask equipped with a stir bar and a vacuum adapter were charged 4.58 g (2.00×10^{-4} mol) PS-PIB-PS (M_n = 22,900 g/mol, MWD = 1.14), 0.020 g (2.0×10^{-4} mol) Cu(I)Cl, 9.2 mL toluene, 3.6 mL (4.0×10^{-2} mol) MA, and 0.043 mL (2.1×10^{-4} mol) PMDETA. The reactor was chilled with $N_{2(l)}$, evacuated, and thawed. This freeze-pump-thaw cycle was repeated a total of three times to remove O_2, after which the reactor was placed into an oil bath heated at 90°C. Aliquots (0.1 mL) for monomer conversion and kinetic analysis were removed at predetermined times via a $N_{2(g)}$ purged syringe. At a predetermined time, the reactor was immersed into $N_{2(l)}$ to quench the polymerization, and 15 mL CH_2Cl_2 was added to dissolve the polymer. The Cu catalyst was removed by stirring the polymer solution with an excess of DOWEX MSC-1 followed by filtering the solution through neutral alumina. The polymer was obtained by precipitation into methanol and was dried under vacuum at 25°C for several days (M_n = 28,000 g/mol, PDI = 1.13).

Monomer conversion was determined using ^{1}H-NMR spectroscopy by monitoring the decrease in the area of one or more selected vinyl resonances, A_{vinyl}, (e.g., one proton at 5.60–5.90 ppm for MA) relative to the sum of the areas of the $-O-CH_3$ or $-O-CH_2-$ protons in the polymer and monomer, A_{P+M}, (3.5–4.2 ppm) at predetermined time intervals using Equation (1).

$$\%\,\text{Monomer Conversion} = \frac{A_{vinyl}/\#\,\text{of protons})}{(A_{P+M}/\#\,\text{of protons})} \cdot 100\% \quad (1)$$

The peak areas were divided by the number of protons that contributed to the respective area. For example, in a methyl acrylate polymerization, A_{P+M} and A_{vinyl} represent proton values of three and one, respectively.

The aliquots were subsequently passed through a column of neutral alumina, vacuum dried at 50°C, and analyzed by SEC. Polymerizations and monomer conversion analysis for the BA and MMA polymerizations were performed in a similar fashion.

Results and Discussion

Synthesis and Characterization of PIB-PS and PS-PIB-PS BCP ATRP Macroinitiators

Previous literature reports have shown that macroinitiators with *sec*-benzyl chloride end groups, including PIB end-capped with a few styrene monomer units (Sty-PIB-Sty), can be efficient macroinitiators for the ATRP of a variety of monomers (14, 15). In this report, PIB-PS and PS-PIB-PS BCPs were prepared by sequential monomer addition using TMPCl or a difunctional cumyl-type initiator (bDCC) at −70°C in a MCHex/MeCl (60/40 v/v) solvent system with an electron donor (DMP) and a proton trap (DTBP) as Lewis base additives in a ratio of 3:1 (v/v), respectively. Polymerization was commenced by the addition of neat $TiCl_4$ co-initiator at ambient temperature (25°C), and after >99% conversion of IB, a 2 M charge of styrene in MCHex/MeCl was added to the quasi-living PIB chains. After ~50% styrene conversion, the polymerization was quenched with prechilled methanol (−70°C). The styrene polymerization was limited to 50% monomer conversion to maximize the chain end functionality of the final block copolymers. SEC analysis indicated that the BCPs possessed molecular weights that were close to the theoretical values and low PDIs (Table 1). End-group analysis using a combination of SEC and ^{1}H-NMR showed that the number average chain end functionalities (F_n), defined as (moles *sec*-benzyl chloride chain ends/moles polymer molecules) were close to the theoretical values. These results indicate that the carbocationic polymerizations were characterized by high blocking efficiency and absence of protic initiation.

ATRP of Acrylic Monomers from PIB-PS and PS-PIB-PS Macroinitiators

The block copolymers described in Table 1 were used as macroinitiators for ATRP of various acrylic monomers. Experimental details and molecular weights of the resulting terpolymers are listed in Table 2.

Table 1
SEC Results for PIB-PS and PS-PIB-PS block copolymers

	PIB				Block copolymer			
Sample ID	Initiator	$M_{n,theo}$ (g/mol)	$M_{n,exp}$ (g/mol)	PDI	$M_{n,theo}$[a] (g/mol)	$M_{n,SEC}$ (g/mol)	PDI	F_n[b]
A	TMPCl	14,900	13,700	1.07	19,800	20,800	1.15	1.1
B	bDCC	5,180	5,540	1.08	10,300	13,300	1.40	1.7
C	bDCC	14,900	15,800	1.04	19,900	22,900	1.14	2.0

[a]Assuming 50% styrene conversion.
[b]$F_n = 5 \times$ (combined DP of PS blocks) $\times$ (area sec-benzyl chloride proton/area aromatic protons).

Table 2
Results from ATRP of various monomers using PIB-PS or PS-PIB-PS macroinitiators

Sample ID	Macro-initiator	Monomer	Ligand	$M_{n,theo}$[a] (g/mol)	$M_{n,SEC}$ (g/mol)	PDI	Time (min)	Monomer conversion %
1	A	MA	PMDETA	28,800	26,800	1.15	240	46
2	B	MA	PMDETA	20,200	20,300	1.48	140	79
3	C	MA	PMDETA	28,800	28,000	1.13	240	36
4	C	MA	Me_6TREN	30,000	30,100	1.14	240	43
5	B	BA	PMDETA	22,900	21,800	1.46	140	74
6	C	BA	PMDETA	26,100	27,000	1.12	120	12
7	C	BA	Me_6TREN	34,500	34,100	1.18	240	46
8	B	MMA	PMDETA	19,800	18,900	1.55	140	67
9	C	MMA	PMDETA	32,800	34,100	1.43	120	49
10	C	MMA	Me_6TREN	28,900	29,500	1.24	120	30

[a] $M_{n,theo} = M_{n,macroinitiator} +$ (mass acrylic monomer/moles macroinitiator) $\times$ (acrylic monomer conversion).

ATRP of Methyl Acrylate from PIB-PS-PIB-PS Macroinitiators

MA was polymerized using a macroinitiator (chain end concentration, $[CE]_0 = 0.012$ M) under ATRP conditions using a Cu(I)Cl/PMDETA catalyst system at 90°C. Figure 1a shows the controlled nature of the MA polymerization evidenced by a linear increase in molecular weight with monomer conversion and narrow, constant PDIs throughout the polymerization. The first-order plot for the polymerization (Figure 1b) was linear, indicating a constant number of active polymerization sites without chain termination. The apparent rate constant for the polymerization (slope of the first-order plot) was approximately $4 \times 10^{-5}\ s^{-1}$. SEC traces of aliquots taken during the polymerization showed a gradual shift to lower elution volumes with time, without any indication of thermally initiated homopolymer (Figure 1c).

The structure of the PIB-PS-PMA block copolymer was elucidated using ^{1}H-NMR spectroscopy (Figure 2). In addition to the protons from the PIB-PS macroinitiator, the methoxy (a, 3.65 ppm) and main chain backbone protons (b, 2.30 ppm) from the PMA block segment were observed. Initiation was quantitative, within the limits of detection by ^{1}H-NMR spectroscopy, as evidenced by the complete disappearance of the *sec*-benzyl chloride proton peak at 4.35 ppm and the appearance of the acrylate chloride proton peak (c, 4.20 ppm). Close agreement between theoretical molecular weights provided further evidence for quantitative initiation.

Using the monofunctional polymerization as a procedural template, polymerizations of MA were initiated from two different PS-PIB-PS macroinitiators (Table 1, Samples B

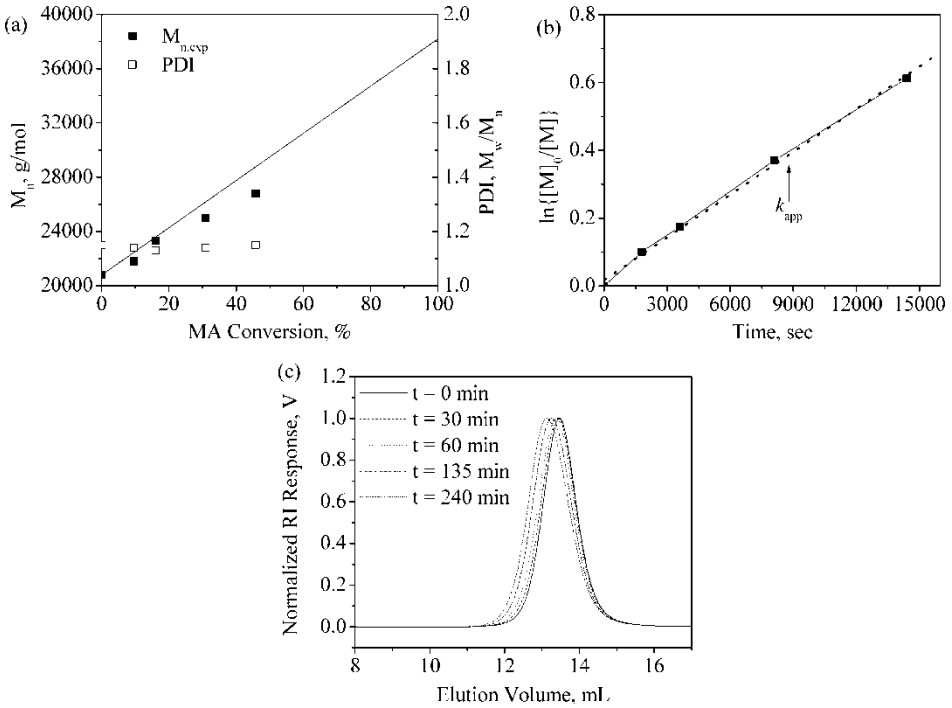

Figure 1. ATRP of MA from PIB-PS macroinitiator in toluene at 90°C (Table 2, Sample 1): (a) M_n and PDI vs. conversion plot (line is theoretical), (b) first-order plot, and (c) SEC traces. $[MA]_0 = 2.51$ M, $[CE]_0 = 0.012$ M, $[Cu(I)Cl]_0 = 0.013$ M, $[PMDETA]_0 = 0.013$ M.

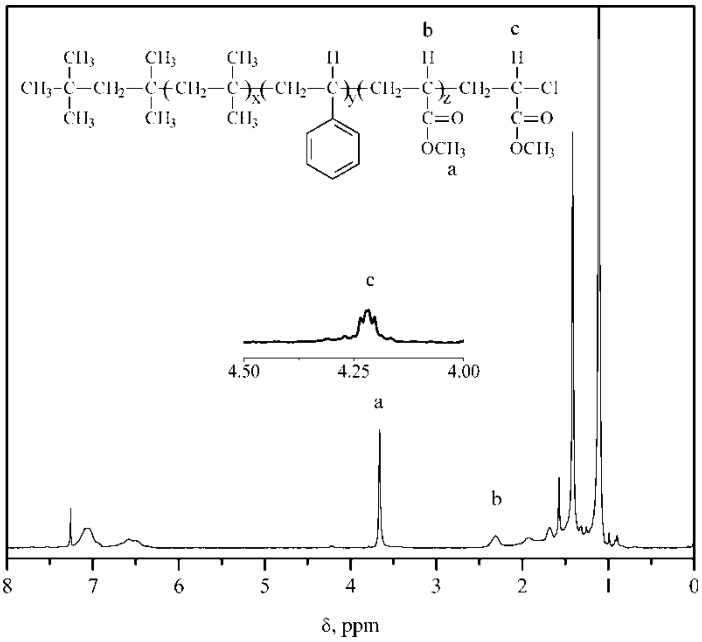

Figure 2. ^{1}H-NMR spectrum of PIB-PS-PMA (Table 2, Sample 1).

and C) at 90°C using Cu(I)Cl/PMDETA in toluene; these two polymerizations differed principally in $[CE]_0$. The polymerizations were heterogeneous, presumably from the formation of the insoluble Cu(II) catalyst species. M_n and PDI vs. conversion plots are shown in Figure 3a. A linear increase in molecular weights with monomer conversion and relatively narrow PDIs were observed in both polymerizations. The final molecular weights were close to theoretical, indicating high initiator efficiency. The first order plots for the polymerizations (Figure 3b) were approximately linear indicating a constant concentration of active species without the presence of irreversible chain termination. From the slopes of the plots, k_{app} was 3×10^{-5} and 2×10^{-4} s^{-1} for $[CE]_0 = 0.024$ and 0.044 M, respectively. These results are consistent with the fact that the latter polymer was produced under conditions of higher molar concentration of PS-PIB-PS chain ends ($[CE]_0$), $[Cu(I)Cl]_0$, and $[PMDETA]_0$. SEC traces of aliquots removed at various times from the reactor (Figure 3c, $[CE]_0 = 0.044$ M) shifted to lower elution volumes with increasing monomer conversion.

MA polymerizations were also conducted with Me_6TREN to observe the effect of catalyst structure on the molecular weight, PDI, and rate of polymerization. Figure 4 compares the M_n and PDI vs. conversion and first-order plots for Me_6TREN and PMDETA MA polymerizations. Using either ligand, the molecular weights increased linearly with monomer conversion, and the PDIs were relatively narrow and were constant during the polymerizations. The Me_6TREN polymerization was faster than the PMDETA polymerization initially but exhibited downward curvature with increased polymerization time. Most controlled polymerizations of acrylates by ATRP use PMDETA and do not require the strongly ligating Me_6TREN. It is hypothesized that the Cu(I)Cl/Me_6TREN catalyst is highly efficient at activating the initiator chain end, resulting in a fast initial polymerization. However, the higher initial concentration of radicals results in increased

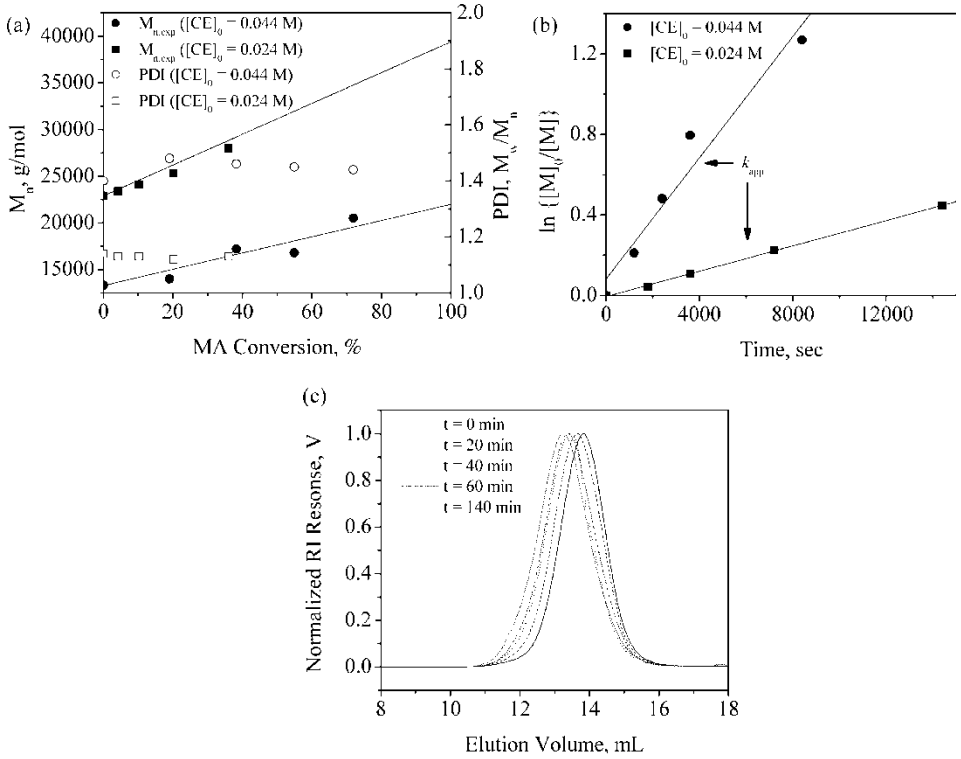

Figure 3. ATRP of MA from different PS-PIB-PS macroinitiators (different $[CE]_0$) in toluene at 90°C (Table 2, Samples 2 and 3): (a) M_n and PDI vs conversion (lines are theoretical), (b) first-order plots, and (c) SEC traces (Sample 2 only). Sample 2: $[MA]_0 = 2.22$ M, $[CE]_0 = 0.044$ M, $[Cu(I)Cl]_0 = 0.022$ M, $[PMDETA]_0 = 0.022$ M. Sample 3: $[MA]_0 = 2.30$ M, $[CE]_0 = 0.024$ M, $[Cu(I)Cl]_0 = 0.012$ M, $[PMDETA]_0 = 0.012$ M.

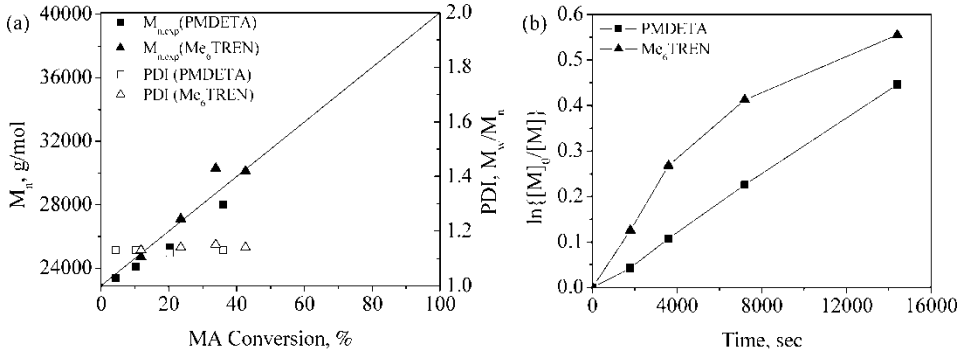

Figure 4. ATRP of MA from PS-PIB-PS macroinitiator in toluene at 90°C using either PMDETA (Table 2, Sample 3) or Me_6TREN (Table 2, Sample 4) as ligand: (a) M_n vs conversion (line is theoretical) and (b) first-order plots. $[MA]_0 = 2.30$ M, $[CE]_0 = 0.024$ M, $[Cu(I)Cl]_0 = 0.012$ M, $[PMDETA]_0$ or $[Me_6TREN]_0 = 0.012$ M.

radical-radical termination reactions and decreased [CE]. These termination reactions result in the formation of $Cu(II)Cl_2/Me_6TREN$, which affects the dormant-active chain equilibrium of the polymerization, resulting in a further slowing of the rate of polymerization (i.e., downward curvature in the first-order plot). This was evidenced in ^{1}H-NMR by the disappearance of the initiator chain end with time (Figure 5). The PMDETA polymerization had a slow decrease of the *sec*-benzyl chloride chain with time; however, in contrast, the *sec*-benzyl chloride chain end resonance was not present in the t = 30 min aliquot in Me_6TREN polymerization. This indicated that the latter polymerization had fast initiation, which increased the initial concentration of radicals early in the polymerization. It is interesting to note that slow initiation in the PMDETA polymerization had no effect on the molecular weights early in the polymerization.

ATRP of Butyl Acrylate from PS-PIB-PS Macroinitiators

ATRP of BA was also conducted using both PS-PIB-PS macroinitiators. For the larger macroinitiator (Table 1, Sample C) ($[CE]_0 = 0.0202$ M), polymerizations were performed using both $Cu(I)Cl/PMDETA$ and $Cu(I)Cl/Me_6TREN$. Figure 6 shows M_n and PDI vs conversion plots. The polymerizations exhibited a linear increase in molecular weight with conversion and had relatively narrow PDIs, regardless of the catalyst system used. The PDIs increased slightly with conversion, possibly from radical-radical coupled products. The polymerization initiated from the smaller macroinitiator, using PMDETA as a ligand ($[CE]_0 = 0.038$ M), displayed the fastest rate of polymerization (Figure 7) because of higher $[CE]_0$, $[Cu(I)Cl]_0$, and $[PMDETA]_0$. All plots exhibited downward curvature, possibly from chain coupling and/or catalyst deactivation.

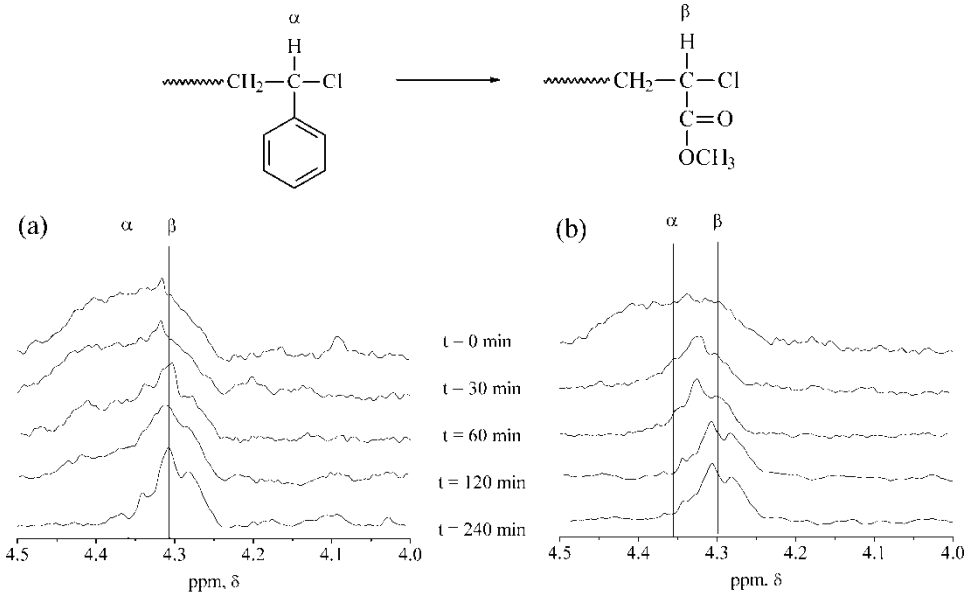

Figure 5. ^{1}H-NMR spectra showing evolution of chain end resonances from *sec*-benzyl chloride (a) to acrylate-chloride, (b) during ATRP of MA from PS-PIB-PS macroinitiator in toluene at 90°C using either PMDETA (left, Table 2, Sample 3) or Me_6TREN (right, Table 2, Sample 4) as ligand.

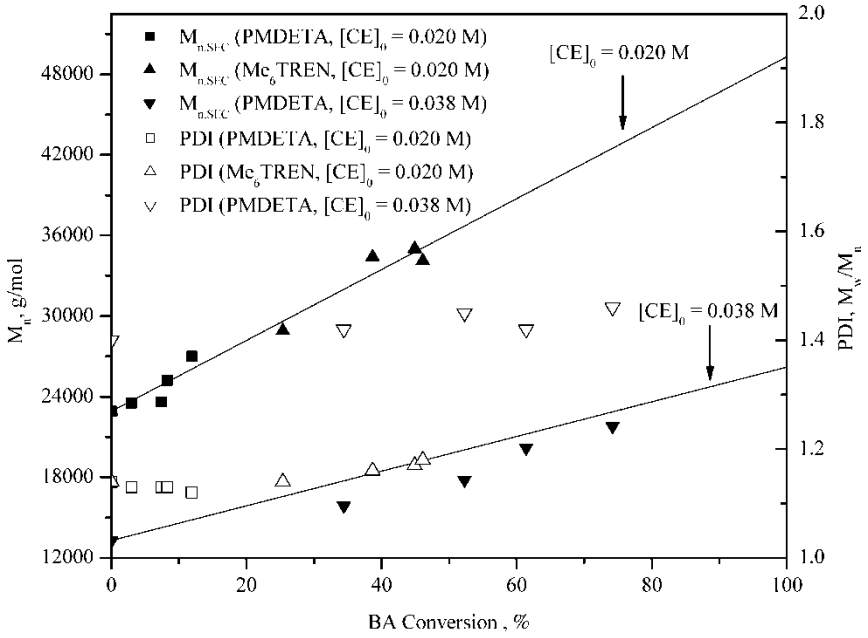

Figure 6. M_n and PDI vs. conversion plots for ATRP of BA from PS-PIB-PS macroinitiators in toluene at 90°C using either PMDETA (Table 2, Samples 5 and 6) or Me_6TREN (Table 2, Sample 7) as ligand. Samples 6 and 7: $[BA]_0 = 2.05$ M, $[CE]_0 = 0.020$ M, $[Cu(I)Cl]_0 = 0.010$ M, $[PMDETA]_0$ or $[Me_6TREN]_0 = 0.010$ M. Samples 5: $[BA]_0 = 1.90$ M, $[CE]_0 = 0.038$ M, $[Cu(I)Cl]_0 = 0.019$ M, $[PMDETA]_0 = 0.019$ M.

The catalyst structure also effected the polymerization of BA. Comparing the $[CE]_0 = 0.020$ M polymerizations, the Cu(I)Cl/Me_6TREN catalyst system had the faster polymerization, similar to the MA polymerizations. The expansion of the chain end region in the ^{1}H-NMR spectrum of the BA polymerization using Me_6TREN revealed the fast disappearance of the *sec*-chloride chain ends (Figure 8). In fact, polymerization was observed in the t = 0 min aliquot, which was taken at room temperature (~25° C). The polymerization was initially fast, but then became very slow. The final two aliquots in the Me_6TREN polymerization (t = 120 and 240 min) had approximately the same conversion (Figure 6), which indicated that polymerization was no longer occurring. This was further evidenced by the first-order plot having a slope essentially equal to zero at higher polymerization times. Because conversion, molecular weight, and PDI of the final two aliquots were essentially the same, it was hypothesized that the polymerization stopped because of a decrease in the catalyst concentration and a build-up of Cu(II)Cl_2/Me_6TREN, which drove the equilibrium to the dormant state. This is further evidenced in ^{1}H-NMR by the presence of the acrylate chloride proton peak in the final aliquot (Figure 8).

ATRP of Methyl Methacrylate from PS-PIB-PS Macroinitiators

The polymerization of MMA using the PS-PIB-PS macroinitiators was less controlled than the acrylate polymerizations. Methacrylates have higher equilibrium constants for ATRP chain-end activation-deactivation compared to acrylates, which tends to promote

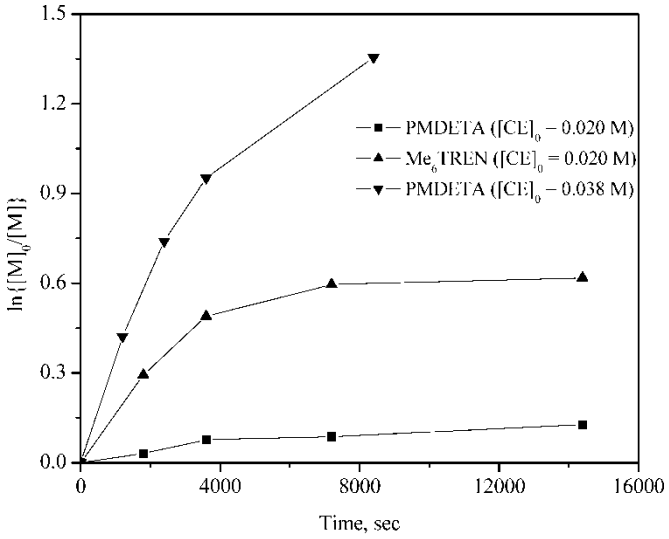

Figure 7. First-order plots for ATRP of BA from PS-PIB-PS macroinitiators in toluene at 90°C using either PMDETA (Table 2, Samples 5 and 6) or Me_6TREN (Table 2, Sample 7) as ligand. Conditions were the same as in Figure 6.

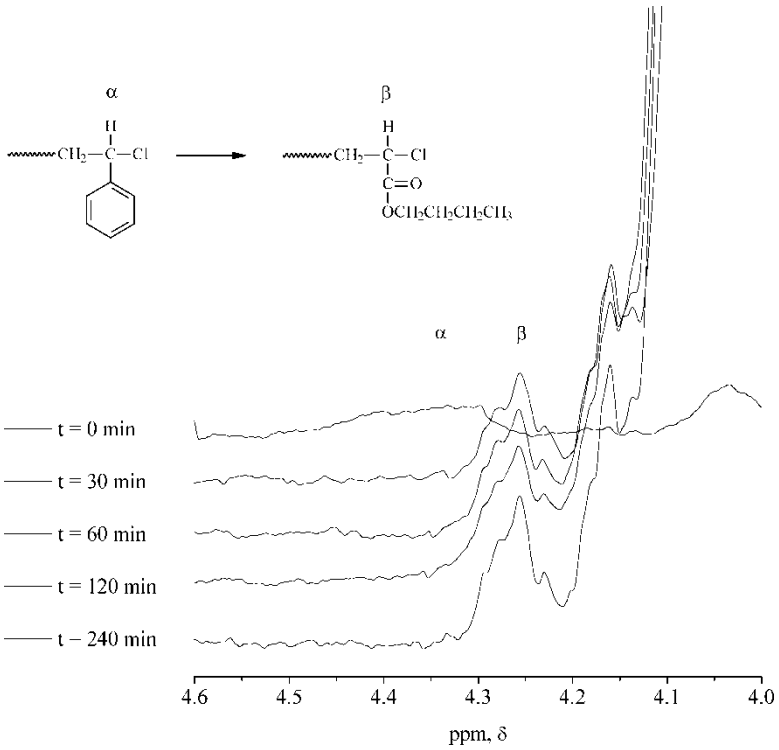

Figure 8. ^{1}H-NMR spectra showing evolution of chain end proton resonances from *sec*-benzyl chloride (a) to acrylate-chloride (b) during ATRP of BA from PS-PIB-PS macroinitiator in toluene at 90°C using Me_6TREN as ligand (Table 2, Sample 7).

irreversible chain termination. In addition, inefficient initiation was observed for the polymerization of MMA initiated by 1-phenylethyl chloride, (22) which is analogous to the PS-PIB-PS chain end structure. In this work, ATRP of MMA was performed using either PMDETA or Me_6TREN with Cu(I)Cl at 90°C. During the polymerizations, the catalyst complexes were heterogeneous in the polymerization medium, and the initial rates of polymerization were faster using PMDETA. Figure 9a shows a linear increase in molecular weight with conversion, but all values were above theoretical, indicating poor initiating efficiency. The PDIs also increased with monomer conversion, suggesting chain-terminating reactions. The early occurrence of termination reactions in both systems is supported by curvature in the first-order plots (Figure 9b), which was also observed previously for the polymerization of MMA using either a Cu(I)/PMDETA (23) or Cu(I)/Me_6TREN (19) catalyst system.

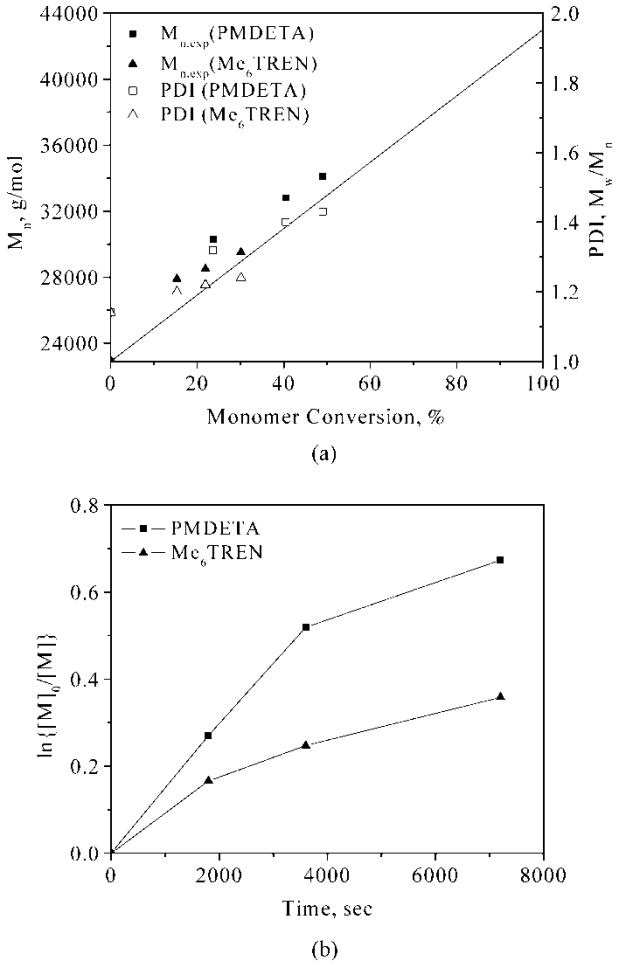

Figure 9. ATRP of MMA from PS-PIB-PS macroinitiator in toluene at 90°C using either PMDETA (Table 2, Sample 9) or Me_6TREN (Table 2, Sample 10) as ligand: (a) M_n and PDI vs conversion (line is theoretical) and (b) first-order plots. $[MMA]_0 = 2.20$ M, $[CE]_0 = 0.022$ M, $[Cu(I)Cl]_0 = 0.011$ M, $[PMDETA]_0$ or $[Me_6TREN]_0 = 0.011$ M.

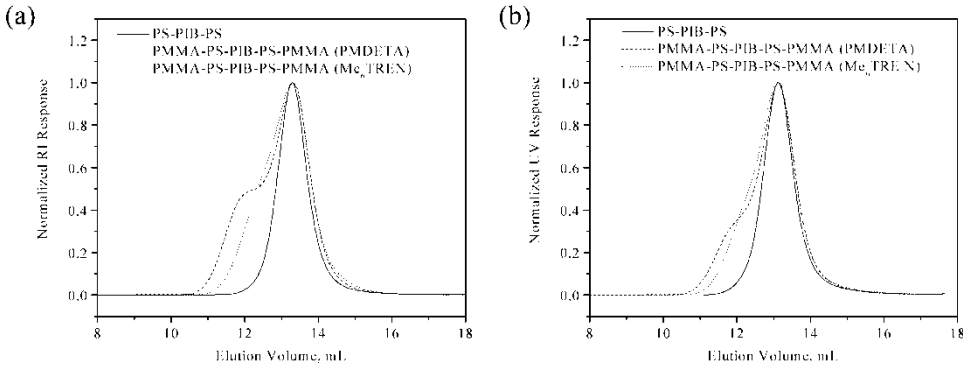

Figure 10. Normalized (a) RI and (b) UV SEC traces for PS-PIB-PS (Table 1, Sample C) and PMMA-PS-PIB-PS-PMMA (Table 2, Samples 9 and 10).

Figure 10 shows the RI (a) and UV (b) SEC traces of the final PMMA-PS-PIB-PS-PMMA block copolymer. The traces clearly show that initiation was incomplete; although a fraction of the PS-PIB-PS did initiate MMA, as evidenced by molecules appearing at lower elution volumes than the PS-PIB-PS macroinitiator. The trace for Sample 9, created using PMDETA, was bimodal. UV analysis showed that both the high molecular weight shoulder and the main peak had a UV signature, indicating that all the chains were initiated from PS-PIB-PS. Finally, ^{1}H-NMR confirmed incomplete initiation by revealing the presence of *sec*-benzyl chloride protons in the final aliquot ($t = 120$ min) of the MMA polymerizations using either PMDETA or Me_6TREN (Figure 11).

Structural and Thermal Characterization of PS-PIB-PS and Pentablock Terpolymers

^{1}H-NMR spectroscopy was used to elucidate the structure of PS-PIB-PS and the pentablock terpolymers (PTP) (Figure 12). Proton resonances in the aromatic (a, 8.0-6.0 ppm) and aliphatic (b-d, 2.1-0.5 ppm) regions were observed in all PTPs, due to the styrene and isobutylene repeat units in the PS-PIB-PS macroinitiator. In addition, each spectrum showed the characteristic resonances from the respective acrylate or methacrylate outer block segments. For example, the spectrum of a PMA-PS-PIB-PS-PMA PTP is shown in Figure 12b; it contains the characteristic methyl acrylate resonances from the methoxy protons (g, 3.7 ppm) and the methine proton α to the carbonyl group (f, 2.3 ppm). Complete initiation of the PS-PIB-PS macroinitiator in the MA and BA polymerizations was indicated by expansion of the chain-end region of the spectra, which showed the presence of a proton resonance due to the acrylate chloride proton peak (h and m, 4.3 ppm), and the absence of the *sec*-benzyl chloride chain end from the macroinitiator. However, initiation of the MMA polymerization was incomplete as evidenced by the presence of the *sec*-benzyl chloride proton in the final block copolymer.

Thermal analysis (TGA and DSC) was performed on PS-PIB-PS and various PTPs and the results are summarized in Table 3. TGA was measured under N_2, and the decomposition temperature, T_d, at 5% mass loss and the inflection T_d were recorded. The latter was taken as the mid-point of the major mass-loss process, determined from

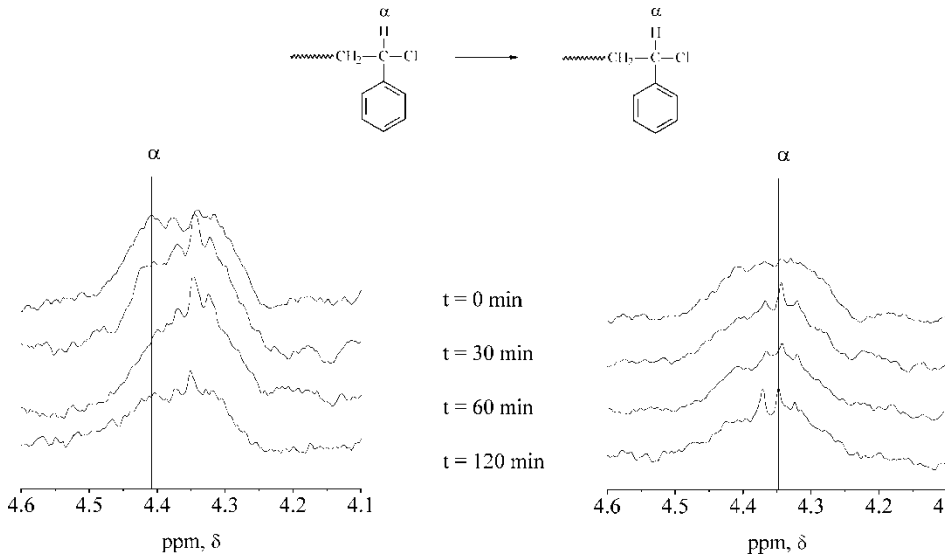

Figure 11. ^{1}H-NMR spectra showing evolution of *sec*-benzyl chloride chain end proton resonance during ATRP of MMA from PS-PIB-PS macroinitiator in toluene at 90°C using either PMDETA (left, Table 2, Sample 9) or Me_6TREN (right, Table 2, Sample 10) as ligand.

the minimum in the first-derivative plot of the thermogram. The T_d at 5% mass loss and inflection T_d in the parent PS-PIB-PS BCP were observed at 343 and 398°C, respectively. These values are slightly lower than those reported by us previously (24). The degradation profiles and respective first-derivative plots for selected pentablock terpolymers are shown in Figure 13. The thermograms for all the samples are similar, but the first-derivative plots revealed subtle differences in the major mass-loss processes for the PTPs. The T_d at 5% mass loss for most of the PTPs was slightly lower than the PS-PIB-PS precursor, and this was attributed to depolymerization and/or release of small molecules of the acrylate or methacrylate block segments. The inflection T_d for all of the PTPs was similar to that of PS-PIB-PS. Thus, incorporation of a polyacrylate block into PS-PIB-PS BCP does not greatly compromise the thermal stability of the final polymer.

DSC thermograms for PS-PIB-PS and various PTPs are shown in Figure 14. The glass transition temperatures (T_g) for the PIB segments in the block copolymers are reported in Table 3; they ranged from −63.0 to −64.8°C, which is in the vicinity of the value for a pure PIB homopolymer and is similar to values previously reported for PS-PIB-PS BCPs (25). Certain PTPs also showed additional glass transitions. The thermograms for PMA-PS-PIB-PS-PMA and PMMA-PS-PIB-PS-PMMA displayed distinct transitions at 13 and 126°C apparently due to the PMA and PMMA blocks, respectively; although the latter value seems slightly high for PMMA. A glass transition for PBA was not visible at −54°C, perhaps because of overlap with the PIB transition. The PS glass transition was not observed by DSC for most of the samples, but was slightly visible in the PMMA-PS-PIB-PS-PMMA thermogram; in general, we have found that the PS transition is difficult to observe using non-modulated DSC when the PS blocks lengths are relatively short as they are here. The presence of several distinctive transitions indicates that the copolymers are phase-separated and that the addition of polar segments to the PS-PIB-PS block copolymers does not affect the segmental mobility of the PIB block segments.

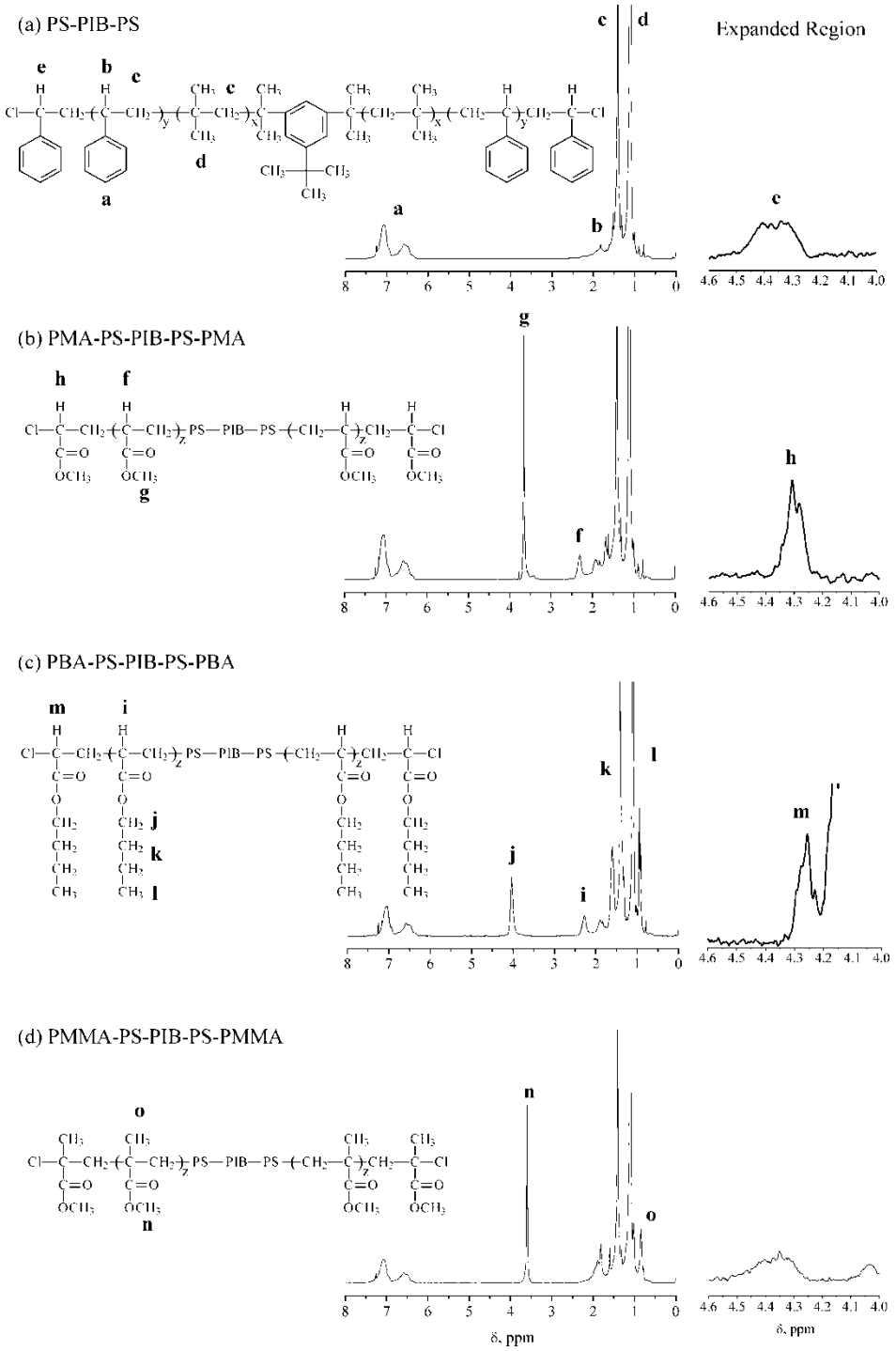

Figure 12. ^{1}H-NMR spectra of (a) PS-PIB-PS (Table 1, Sample C), (b) PMA-PS-PIB-PS-PMA (Table 2, Sample 4), (c) PBA-PS-PIB-PS-PBA (Table 2, Sample 7, and (d) PMMA-PS-PIB-PS-PMMA (Table 2, Sample 10).

Table 3
Thermal analysis results for PS-PIB-PS and various pentablock terpolymers

Sample ID	Sample description	T_d, 5% Mass loss (°C)	Inflection T_d (°C)	PIB T_g (°C)	PIB:PS:X wt%[a]
C	PS-PIB-PS	343	398	−63.5	66:34:0
4	PMA-PS-PIB-PS-PMA	336	406	−63.5	55:24:21
7	PBA-PS-PIB-PS-PBA	320	414	−63.0	64:29:07
6	PMMA-PS-PIB-PS-PMMA	320	398	−64.8	51:22:27

[a]Determined by ^{1}H-NMR.

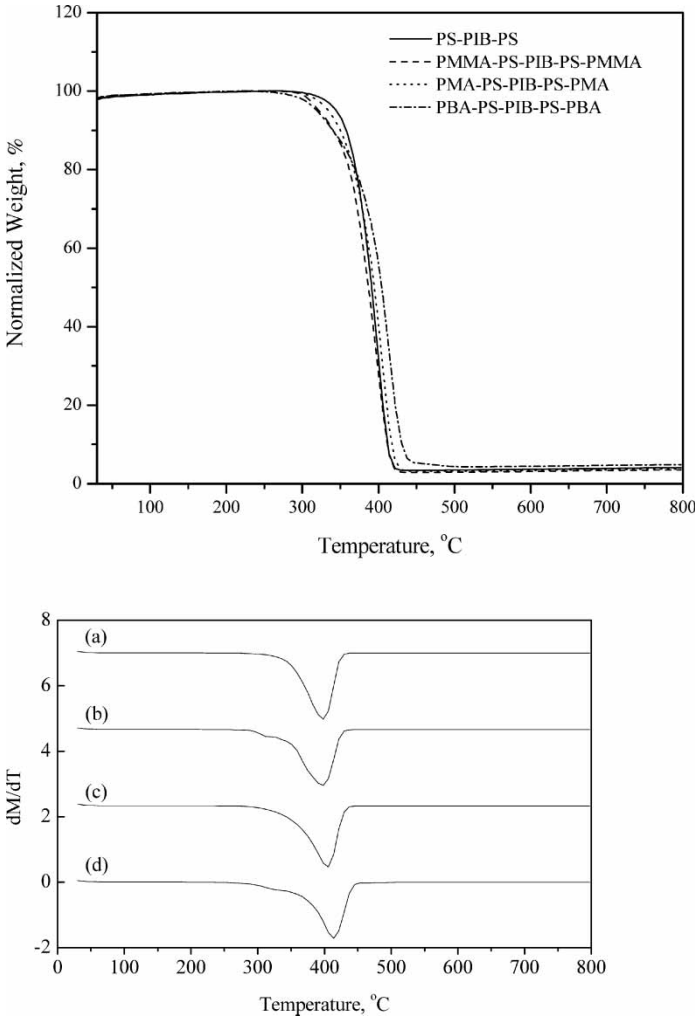

Figure 13. TGA thermograms (top) and first-derivative plots (bottom) of (a) PS-PIB-PS (Table 1, Sample C), (b) PMMA-PS-PIB-PS-PMMA (Table 2, Sample 9), (c) PMA-PS-PIB-PS-PMA (Table 2, Sample 4), and (d) PBA-PS-PIB-PS-PBA (Table 2, Sample 6).

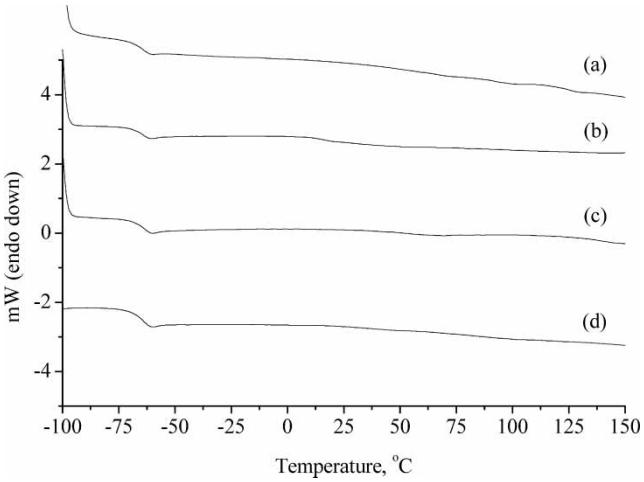

Figure 14. First scan DSC thermograms for (a) PMMA-PS-PIB-PS-PMMA (Table 2, Sample 9), (b) PMA-PS-PIB-PS-PMA (Table 2, Sample 4), (c) PBA-PS-PIB-PS-PBA (Table 2, Sample 6), and (d) PS-PIB-PS (Table 1, Sample C).

Conclusions

Pentablock copolymers having a basic structure of X-PS-PIB-PS-X (where X = PMA, PBA, or PMMA) were synthesized by a combination of QCP and ATRP. The PS-PIB-PS BCPs were well defined having targeted molecular weights, narrow PDIs, and a high F_n with respect to the *sec*-benzyl chloride chain-end functionality. Cu(I)Cl, in conjunction with either PMDETA or Me_6TREN, resulted in well-defined pentablock copolymers. Initiation of MA or BA from the PS-PIB-PS macroinitiator was quantitative, as shown by ^{1}H-NMR and SEC, with the more active ligand, Me6TREN, resulting in faster polymerizations. The polymerization of MMA was less controlled. ^{1}H-NMR spectroscopy indicated incomplete initiation, and the SEC traces of PMMA-PS-PIB-PS-PMMA were very broad and multimodal. Thermal stabilities of the pentablock copolymers were slightly less than the PS-PIB-PS precursor. DSC analysis revealed that the incorporation of the polar outer blocks did not affect the T_g of the PIB segments. This observation, along with the fact that several of the pentablock copolymers displayed multiple glass transitions, indicated that the systems were phase separated.

Acknowledgements

Support from DEPSCoR (ARO) Grant No. DAAD19-02-1-0155 and the National Science Foundation Materials Research Science and Engineering Center (DMR 0213883) is gratefully acknowledged.

References

1. Kaszas, G., Puskas, J.E., and Kennedy, J.P. (1988) *Makromol. Chem., Macromol. Symp.*, 13/14: 473.
2. Storey, R.F., Curry, C.L., and Hendry, L.K. (2001) *Macromolecules*, 34: 5416.
3. Gyor, M., Wang, H.C., and Faust, R. (1992) *J. Macromol. Sci., Pure Appl. Chem.*, A29: 639.

4. Kwon, Y. and Faust, R. (2004) *Adv. Polym. Sci.*, 167: 107.
5. Zhou, Y., Faust, R., Richard, R., and Schwarz, M. (2005) *Macromolecules*, 38: 8183.
6. Fang, Z. and Kennedy, J.P. (2002) *J. Polym. Sci.: Part A: Polym. Chem.*, 40: 3662.
7. Fang, Z. and Kennedy, J.P. (2002) *J. Polym. Sci.: Part A: Polym. Chem.*, 40: 3679.
8. Moustafa, A.F., Fang, Z., and Kennedy, J.P. (2002) *Polym. Bull.*, 48: 225.
9. Kennedy, J.P., Price, J.L., and Koshimura, K. (1991) *Macromolecules*, 24: 6567.
10. Breland, L.K., Murphy, J.C., and Storey, R.F. (2006) *Polymer*, 47: 1852.
11. Hong, S.C., Pakula, T., and Matyjaszewski, K. (2001) *Macromol. Chem. Phys.*, 202: 3392.
12. Truelsen, J.H., Kops, J., and Batsberg, W. (2000) *Macromol. Rapid Commun.*, 21: 98.
13. Takacs, A. and Faust, R. (1996) *J.M.S.-Pure & Appl. Chem.*, A33: 117.
14. Coca, S. and Matyjaszewski, K. (1997) *J. Polym. Sci.: Part A: Polym. Chem.*, 35: 3595.
15. Chen, X., Ivan, B., Kops, J., and Batsberg, W. (1998) *Macromol. Rapid Commun.*, 19: 585.
16. Storey, R.F., Scheuer, A.D., and Achord, B.C. (2005) *Polymer*, 46: 2141.
17. Kopchick, J., Storey, R.F., and Mauritz, K.A. to be published.
18. Storey, R.F., Chisholm, B.J., and Masse, M.A. (1996) *Polymer*, 37: 2925.
19. Queffelec, J., Gaynor, S.G., and Matyjaszewski, K. (2000) *Macromolecules*, 33: 8629.
20. Storey, R.F., Stokes, C.D., and Harrison, J.J. (2005) *Macromolecules*, 38 (11): 4618.
21. Storey, R.F., Curry, C.L., and Hendry, L.K. (2001) *Macromolecules*, 34: 5416.
22. Matyjaszewski, K., Wang, J.L., Grimaud, T., and Shipp, D.A. (1998) *Macromolecules*, 31: 1527.
23. Snijder, A., Klumperman, B., and van der Linde, R. (2002) *Macromolecules*, 35: 4785.
24. Reuschle, D.A., Ali, N., Mauritz, K.A., Brister, L.B., Maggio, T.L., and Storey, R.F. (1999) *ACS Div. Polym. Chem., Polym. Preprs.*, 40: 715.
25. Mauritz, K.A., Storey, R.F., Mountz, D.A., and Reuschle, D.A. (2002) *Polymer*, 43: 4315.